*Rapports internes du LaMSID*

S. GENIAUT – P. MASSIN – N. MOES*

# A stable 3D contact formulation using X-FEM

RI-B3-N°007 2007

*Institut de Recherche en Génie Civil et Mécanique – Ecole Centrale de Nantes

***Laboratoire de Mécanique des Structures Industrielles Durables***
*UMR EDF-CNRS 2832*
*EDF R&D*
*1, Avenue du Général de Gaulle - 92141 CLAMART CEDEX FRANCE*

# A stable 3D contact formulation using X-FEM

**Samuel Geniaut*,** — Patrick Massin* — Nicolas Moës****

** Laboratoire de Mécanique des Structures Industrielles Durables*
*CNRS-EDF, UMR 2832*
*1, avenue du Général de Gaulle, 92141 Clamart*
*{patrick.massin, samuel.geniaut}@edf.fr*

*** Institut de recherche en Génie civil et Mécanique*
*École Centrale de Nantes/Université de Nantes/UMR CNRS 6183*
*1, rue de la Noé, 44321 Nantes Cedex 3*
*nicolas.moes@ec-nantes.fr*

ABSTRACT. *This paper presents a 3D non-locking contact approach, within the eXtended Finite Element Method (X-FEM) framework. X-FEM allows one to introduce interface independently of the mesh. The contact problem on the interface leads to an Augmented Lagrangian formulation derived from the discretization of its continuous formulation. It is shown that a simple choice of the Lagrange multiplier space is not suitable and leads to contact pressure oscillations. An algorithm for the restriction of the Lagrange multiplier approximation space is proposed to stabilize the formulation. The stability of the mixed displacement-contact pressure formulation is discussed in terms of convergence of the energy error. Numerical examples performed with the Finite Element software Code_Aster illustrate this approach while solving three-dimensional problems with contact.*

KEYWORDS: *X-FEM, adhesive contact, 3D.*

REMN – 15/2006. Calculs avec méthodes sans maillage, pages 1 à X

## 1. Introduction

The eXtented Finite Element (Moës *et al.*, 1999) approach allows meshes not to respect the crack geometry. This method has managed to combine performances and robustness, considering non-meshed cracks in a finite element framework. X-FEM uses the Partition of Unity and enriches the classical basis of shape functions with discontinuous functions. The discontinuity of the displacement field across the crack surface is then introduced by a generalised Heaviside function, and adding asymptotic fields at the front crack gives good precision in linear elastic fracture mechanics. The main advantage of X-FEM in comparison to mesh-less methods is its easy implementation in a general finite element software, and its capacities to be applied to various fields: large transformations (Legrain *et al.*, 2005), plasticity (Elguedj *et al.*, 2006)… One can say that X-FEM extends the possibilities of the FEM, keeping all its advantages. A useful amelioration has been proposed by (Sukumar *et al.*, 2001*)* with the introduction of level set functions to represent discontinuities (cracks, voids,…). This approach is extremely handy in 3D to treat crack propagation (Gravouil *et al.*, 2002).

In this paper, we propose an X-FEM approach with contact on the interface. Adhesion, obtained from a frictional law, is used in order to validate our analysis, restricted so far to contact and adhesive contact, with respect to analytical results. Only few works have been published on that subject, and all of them are addressed to 2D problems. In (Dolbow *et al.*, 2001), a 2D crack problem with frictional contact is treated, with a formulation close to the Augmented Lagrangian Method (Alart *et al.*, 1991). Following the work of Dolbow *et al.*, Ribeaucourt *et al.* study rolling fatigue and takes into account frictional contact on the surfaces of a 2D fatigue crack (Ribeaucourt *et al.*, 2005). Not directly related to contact problems, two papers concern the difficulty to impose conditions on an interface with X-FEM. In (Ji *et al.*, 2004) the authors observe oscillations of the Lagrange multipliers used to impose interfacial conditions. In (Moës *et al.*, 2005), an algorithm is proposed to reduce oscillations of the Lagrange multipliers in 2D. This algorithm, based on geometric considerations, build a Lagrange multiplier space compatible with the displacement approximation space.

In our extension to 3D contact problem with X-FEM, we present an amelioration of the previous algorithm which leads to a non-locking contact formulation. We have chosen a framework close to the Augmented Lagrangian Method, derived form a continuum mechanics formulation of contact proposed by (Ben Dhia *et al.*, 2000). Whereas discrete approaches consider the contact problem as a direct modification of nodal forces, the equations are discretized within the finite element method framework leading to an assembly of elementary contributions. For these "continuous" methods, developed also by (Laursen *et al.*, 1993) (Curnier *et al.*, 1995), the contact conditions are seen as an interface law and not as boundary conditions. With the discretization, the notion of contact element appears and the

non-differentiable contact law can be treated via an hybrid element (Ben Dhia *et al.*, 2002) including contact efforts in the problem unknowns. In the method proposed by Ben Dhia, the non-differentiability of the contact is treated by an algorithm of active constraints (Dumont, 1995), and the non-differentiability due to the friction is solved using a fixed point method on the friction threshold (see Zarroug, 2002, for more details).

With X-FEM, the two sides of the interface are viewed as a single surface which may cut a finite element. The integration of the contact terms on that non-meshed surface calls upon quantities related to the nodes belonging to the elements that are cut by the interface. Besides, one of the main features of contact with X-FEM is that under small displacement assumptions, no contact-nodes searching algorithm is needed, because a geometrical point on the surface can be seen as two physical points, one on each side of the surface. The displacement jump is therefore just expressed in terms of the enriched degrees of freedom introduced by X-FEM.

This paper is composed of 5 sections. After this brief introduction, in section 2, the 3D frictional contact problem with adhesion is introduced. The general equations, the contact and the friction laws are recalled. Section 3 presents the mixed displacement-contact pressure variational formulation associated. In section 4, the discretization of the displacement and the contact pressure fields is described leading to an hybrid extended finite element. Section 5 studies the stability of the mixed formulation, illustrated on numerical examples.

## 2. Presentation of the frictional contact problem with adhesion

This part briefly recalls the non-linear equations of the frictional contact problem. We consider the quasi-static response of a cracked body $\Omega \subset \Re^3$, under prescribed body forces $\mathbf{f}$ and prescribed tractions $\mathbf{t}$ on $\Gamma_t$. The structure is clamped on $\Gamma_u$. The outward unit normal of $\partial\Omega$ is denoted by $\mathbf{n_{ext}}$. Considering a smooth extension of the crack $\Gamma_C$, we separate $\Omega$ in two bodies $\Omega^i$, i = 1,2 and we designate $\mathbf{n^i}$ the outward unit normals of each crack surface $\Gamma^i$, and $\mathbf{r^i}$ the effort densities due to potentially frictional contact interactions between the two surfaces.

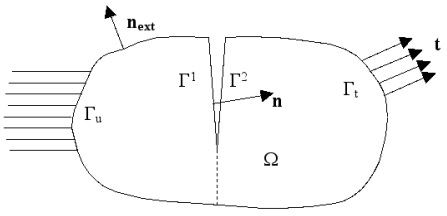


**Figure 1.** *Notation for the frictional contact problem.*

In the framework of small displacements, the constitutive law for the elastic linear material is given by:

$$\boldsymbol{\sigma} = \mathbf{C}\boldsymbol{\varepsilon} \text{ in } \Omega \quad [1]$$

where $\mathbf{C}$ is the Hooke tensor and $\boldsymbol{\varepsilon}$ the symmetrical part of the gradient of $\mathbf{u}$. Using the former notations, the equilibrium equations and the boundary conditions are:

$$\begin{cases} \nabla \cdot \boldsymbol{\sigma} = \mathbf{f} \quad \text{in } \Omega \\ \boldsymbol{\sigma} \cdot \mathbf{n}_{\text{ext}} = \mathbf{t} \quad \text{on } \Gamma_t \\ \boldsymbol{\sigma} \cdot \mathbf{n}^{\mathbf{i}} = \mathbf{r}^{\mathbf{i}} \quad \text{on } \Gamma^i \quad i = 1,2 \\ \mathbf{u} = \mathbf{0} \quad \text{on } \Gamma_u \end{cases} \quad [2]$$

Let p be a point of $\Gamma_c$. We denote $p^1$ and $p^2$ the points initially coinciding on $\Gamma^1$ and $\Gamma^2$ respectively, and $[[\mathbf{x}]]$ the displacement jump across the interface. The non-interpenetration condition between $p^1$ and $p^2$ is written following the direction of the outward normal to $\Gamma^1$ $\mathbf{n} = \mathbf{n}^1$:

$$d_n = [[\mathbf{x}]] \cdot \mathbf{n} = \left(\mathbf{x}\left(p^1\right) - \mathbf{x}\left(p^2\right)\right) \cdot \mathbf{n} \leq 0 \quad [3]$$

Figure 2 shows how the frictional contact effort density $\mathbf{r}$ is decomposed in a normal contribution $\lambda$ which corresponds to the normal contact pressure, and a tangential one $\mathbf{r}_\tau$. The frictional contact effort density can be written as follows:

$$\mathbf{r} = \mathbf{r}^1 = -\mathbf{r}^2 = \lambda \mathbf{n} + \mathbf{r}_\tau \quad [4]$$

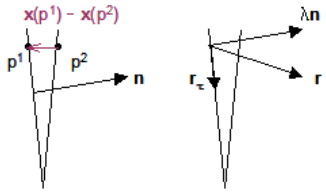


**Figure 2.** *Definitions of the gap and the contact reaction.*

With these notations, contact law (Signorini's laws) yields to:

$$d_n \leq 0\,,\ \lambda \leq 0\,,\ \lambda d_n = 0 \quad [5]$$

Inequations governing unilateral contact, are not well-suited for a weak formulation. This is the reason why [5] is rewritten under an equivalent implicit equation (Ben Dhia *et al.*, 1999):

$$\lambda - \chi(g_n) g_n = 0 \qquad [6]$$

In this equation, which characterises the contact law, $g_n$ is the Augmented contact multiplier (Alart *et al.* 1991) defined by:

$$g_n = \lambda - \rho_n d_n \qquad [7]$$

where $\rho_n$ is a strictly positive constant. The equation [6] is said implicit because it involves $\chi$, the indicative function of $\Re^-$. The function $\chi(x)$ is equal to 1 if $x < 0$ and is equal to 0 if $x \geq 0$.

For frictional effects, we use the classical Coulomb's law, which is a non-differentiable and non-associative law:

$$\begin{aligned} &\|\mathbf{r}_\tau\| \leq \mu|\lambda| \\ &\text{if} \quad \|\mathbf{r}_\tau\| < \mu|\lambda| \quad \text{then} \quad \mathbf{v}_\tau = \mathbf{0} \\ &\text{if} \quad \|\mathbf{r}_\tau\| = \mu|\lambda| \quad \text{then} \ \exists \alpha \geq 0 \ ; \quad \mathbf{v}_\tau = -\alpha \mathbf{r}_\tau \end{aligned} \qquad [8]$$

where $\mu$ is the Coulomb's frictional coefficient and $\mathbf{v}_\tau$ the relative tangential velocity. In the following applications, used to validate our contact formulation, $\mu$ is taken high enough to ensure adhesion.

An equivalent procedure to the one used for the contact law is carried out, in order to obtain an equivalent equation of [8]. We will define by equation [9a] a semi-multiplier of friction $\mathbf{\Lambda}$, which modulus lies between 0 and 1 (strictly lower than 1 in our adhesive case). $\mathbf{\Lambda}$ corresponds to the sliding direction for sliding points when its modulus is equal to one, and $\mathbf{\Lambda}$ corresponds to the adhesion direction when its modulus is strictly lower than one. We introduce then the Augmented semi-multiplier of friction $\mathbf{g}_\tau$ in the equation [9b]. The equation [9a-c] is equivalent to the Coulomb's friction law, where $P_{B(0,1)}$ is the projection on the unit ball and $\rho_\tau$ is a strictly positive parameter (Ben Dhia, 1990):

$$\mathbf{r}_\tau = \mu \lambda \mathbf{\Lambda} \qquad [9a]$$

$$\mathbf{g}_\tau = \mathbf{\Lambda} + \rho_\tau \mathbf{v}_\tau \qquad [9b]$$

$$\mathbf{\Lambda} - P_{B(0,1)}(\mathbf{g}_\tau) = \mathbf{0} \qquad [9c]$$

## 3. Mixed continuous variational formulation

In this section, we recall the weak frictional contact formulation of (Ben Dhia, 2002) used in this work. Displacement fields are chosen in $\boldsymbol{V_0} = \{\mathbf{v} \in \boldsymbol{H^1}$ , $\mathbf{v}$ discontinuous across $\Gamma_c$ , $\mathbf{v} = \mathbf{0}$ on $\Gamma_u\}$ the space of the smooth enough kinematically admissible displacement fields. Let $\boldsymbol{H}$ be the contact pressure space.

Find $(\mathbf{u}, \lambda, \mathbf{\Lambda}) \in \mathbf{V_0} \times H \times \mathbf{H}$

$\forall (\mathbf{v}, \lambda^*, \mathbf{\Lambda}^*) \in \mathbf{V_0} \times H \times \mathbf{H}$

$$\int_\Omega \boldsymbol{\sigma}(\mathbf{u}) : \boldsymbol{\varepsilon}(\mathbf{v}) d\Omega - \int_\Omega \mathbf{f} \cdot \mathbf{v} d\Omega - \int_{\Gamma_t} \mathbf{t} \cdot \mathbf{v} d\Gamma - \int_{\Gamma_c} \chi(g_n) g_n \mathbf{n} \cdot [[\mathbf{v}]] d\Gamma_c - \int_{\Gamma_c} \chi(g_n) \mu \lambda P_{B(0,1)}(\mathbf{g_\tau}) \cdot [[\mathbf{v}]] d\Gamma_c = 0$$

$$\int_{\Gamma c} \frac{-1}{\rho_n} \{\lambda - \chi(g_n) g_n\} \lambda^* d\Gamma_c = 0$$

$$\int_{\Gamma c} \frac{-\mu \chi(g_n) \lambda}{\rho_\tau} \left\{\mathbf{\Lambda} - P_{B(0,1)}(\mathbf{g_\tau})\right\} \mathbf{\Lambda}^* d\Gamma_c + \int_{\Gamma c} (1 - \chi(g_n)) \mathbf{\Lambda} \mathbf{\Lambda}^* d\Gamma_c = 0$$

where the stress tensor $\boldsymbol{\sigma}$ is given by the constitutive law [1], and $g_n$ and $\mathbf{g_\tau}$ are respectively defined by [7] and [9b].

## 4. Discretizations

We define $\mathbf{V_0^h}$, $H^h$ and $\mathbf{H^h}$, the finite dimension sub-spaces of the continuous spaces $\mathbf{V_0}$, H and $\mathbf{H}$, which allow one to approximate the fields $\mathbf{u}$, $\lambda$ and $\mathbf{\Lambda}$.

### 4.1 Displacements approximation with X-FEM

The main idea is to enrich the basis of interpolation with the partition of unity (Melenk *et al.*, 1996). The classical finite element approximation is recalled:

$$\mathbf{u^h}(\mathbf{x}) = \sum_{i \in N_n(\mathbf{x})} \mathbf{a_i} \phi_i(\mathbf{x})$$

where $\mathbf{a_i}$ are the displacement degrees of freedom at node i and $\phi_i$ the shape function associated to node i. $N_n(\mathbf{x})$ is the set of nodes whose support contains the point $\mathbf{x}$.

To represent the displacement jump across $\Gamma_c$, we introduce the generalised Heaviside function (Moës *et al.*, 1999): $H(\mathbf{x})$ is equal to –1 if the point $\mathbf{x}$ is "below"

the crack surface and is equal to 1 if the point **x** is "above" the crack surface. Near the crack front, a special enrichment is added with functions based on the asymptotic developments of displacement fields in linear elastic fracture mechanics. But we will focus in this paper on elements completely cut by the crack (case of interface). The X-FEM displacement approximation is then:

$$\mathbf{u}^{\mathbf{h}}(\mathbf{x}) = \sum_i \mathbf{a}_i \phi_i(\mathbf{x}) + \sum_j \mathbf{b}_j \phi_j(\mathbf{x}) H(\mathbf{x}) \qquad [11]$$

where $\mathbf{b_j}$ are the enriched degrees of freedom. Nodes *j* are the nodes whose cover is completely cut by the crack.

A level set representation of the interface is used within the X-FEM framework (Sukumar *et al.*, 2001). The level set $\psi$ is a signed distance function to the interface. Its sign is arbitrary chosen: $\psi(x) < 0$ for $x \in \Omega^1$ and $\psi(x) > 0$ for $x \in \Omega^2$.

With this approximation, the displacement jump across the interace surface is directly expressed in terms of the degrees of freedom enriched by X-FEM. The expression of the displacement jump contains the discontinuous terms of the displacement approximation [11] and is written as follows:

$$[[\mathbf{v}^{\mathbf{h}}]] = \sum_j -2\phi_j \mathbf{b}_j$$

### 4.2 Contact unknowns approximation

The surface of the cut intersecting an element can be approximated firstly with a polygon (which can have a complex shape, such as non-planar hexagon). To define a FE approximation on that surface, we have decided to cut this polygon in sub-triangles in order to use the classical linear shape functions of the triangle $\phi_i$:

$$\lambda^h(\mathbf{x}) = \sum_{i=1}^{3} \lambda_i \phi_i(\mathbf{x}), \quad \mathbf{\Lambda}^h(\mathbf{x}) = \sum_{i=1}^{3} \mathbf{\Lambda}_i \phi_i(\mathbf{x}) \qquad [12]$$

A similar approximation has been used by (Ji *et al.*, 2004) for problems where interfacial conditions are enforced in a two-phase body. The vertices of the sub-triangles are the intersections between the interface and the edges of the elements. These vertices can be either a point on an edge, or a node. Therefore, the frictional contact unknowns (the contact pressures $\lambda_i$ and the semi-multipliers of friction $\mathbf{\Lambda_i}$ at the vertices of the sub-triangles) are not always real nodal unknowns since the vertices of the sub-triangles are not necessarily included in the mesh. However, in *Code_Aster*, the finite element software developed by EDF for solving general problems in mechanics, unknowns must be nodal ones, as in many finite element softwares. For implementation purpose, if a vertex of a sub-triangle is a point located

on an edge (not a node) then the contact unknowns of that point are associated to the middle node of the edge (see Figure 3).

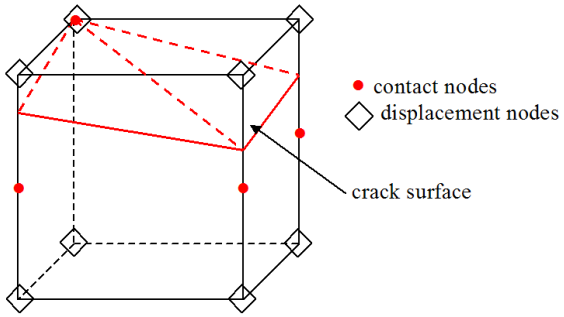


**Figure 3.** *Example of contact sub-triangles and associated unknowns location.*

To sum up, the contact element we propose is based on a quadratic element. Classical and enriched displacement degrees of freedom (*dof*) are on the summit nodes as for classical linear elements. Then, the element has initially contact *dof* at every summit and middle nodes as for classical quadratic elements. Depending on the position of the interface, some of these contact *dof* are contact unknowns (they take part of the discretized equations), while the others are inactive and imposed to zero (they do not take part in the discretized equations).

## 5. Stability of the mixed displacement-contact pressure formulation

One of the features of mixed formulations is that not all combinations of discretizations are stable and only a judicious choice of the finite element spaces will lead to optimal convergence. To assure that, the ellipticity and the inf-sup (or LBB) conditions must be satisfied (Bathe, 2001). Unfortunately, our mixed formulation is not LBB-stable. Indeed, imposing contact conditions on the interface and imposing Dirichlet boundary conditions is quite similar. In (Moës *et al.*, 2005), the question of how imposing essential boundary conditions on an interface with X-FEM is discussed. Dirichlet conditions are imposed *via* Lagrange multipliers on an interface which crosses triangular elements and the mixed formulation shows instabilities. Lagrange multiplier space is too rich and oscillations of the multipliers occur.

The same phenomenon is observed with our formulation of contact with X-FEM. We consider a 3D elastic plate $\Omega$ under non-uniform compression. The inferior face is clamped and a parabolic pressure p(y) is applied on the superior face. $P_{max}$ is taken equal to 1 Pa. An interface $\Gamma$ crosses completely the plate at z = 0.5 m. Frictional contact conditions are applied on the interface, and the Coulomb coefficient is taken high enough to have adherence.

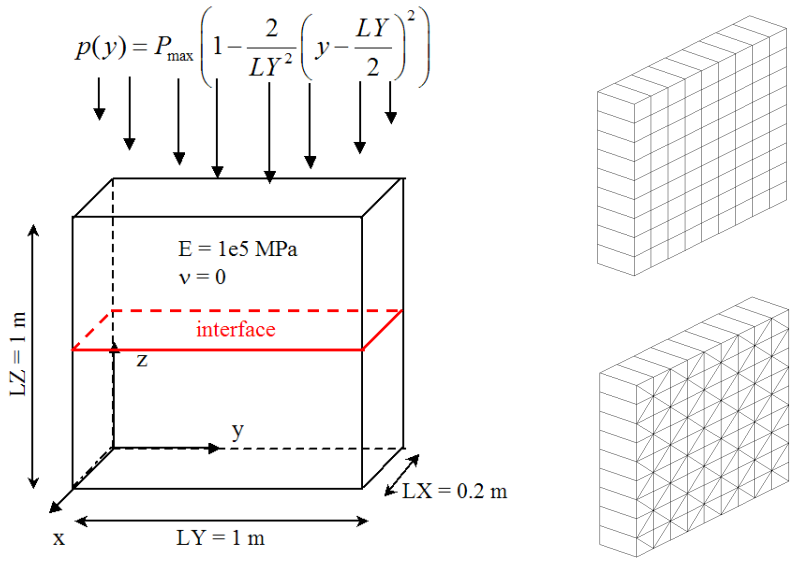


**Figure 4.** *On the left, the geometry of the 3D plate. On the right, the two meshes.*

Two types of regular meshes are studied: one with hexahedrons and one with pentahedrons (prisms), with an odd number of elements in the z direction, so that the interface cuts the elements (see Figure 4). On Figure 5, we compare the contact pressure along the y-axis for both meshes. The size of the elements is denoted by *h*, so that 1/*h* represents the number of elements in the directions y and z (for pentahedrons, the number of elements is in fact 2/*h* in the y-direction). The reference is the analytical solution for contact pressure, which is equal to the prescribed pressure p(y). With hexahedrons in our mesh configuration, the Lagrange multiplier space on the interface is similar to the space obtained by considering an interface coinciding with the edges of the hexahedrons. In this case, the combination of the displacement and multiplier approximation spaces does not lead to locking and the resulting contact pressure is parabolic as expected (Figure 5). However, with pentahedrons, more multipliers are introduced. Those on the diagonal edges make the system over-constrained, and oscillations of the contact pressure occur, as it can be seen on Figure 5. (Ji *et al.*, 2004) also obtained similar oscillations. In (Moës *et al.*, 2005), an algorithm is proposed to reduce the Lagrange multiplier space. The superfluous multipliers are linked to the other multipliers, imposing equality or linear relations between the Lagrange multipliers. For more details, see (Moës *et al.*, 2005). This algorithm tends to impose more equality relations than linear relations, so the linear approximation of the multipliers (equation [12]) is degraded. We have improved this algorithm to make it more efficient and reverse this trend by imposing more linear relations in order to satisfy most of the time equation [12]. We note that

the relations imposed between contact multipliers are also imposed between semi-multipliers of friction in the adhesive case since oscillations also occur on the semi-multipliers of friction. Up to now, in the frictional case where sliding occurs, this choice does not seem to be convenient due to the relation between the tangential and normal pressures, so that further investigations are needed.

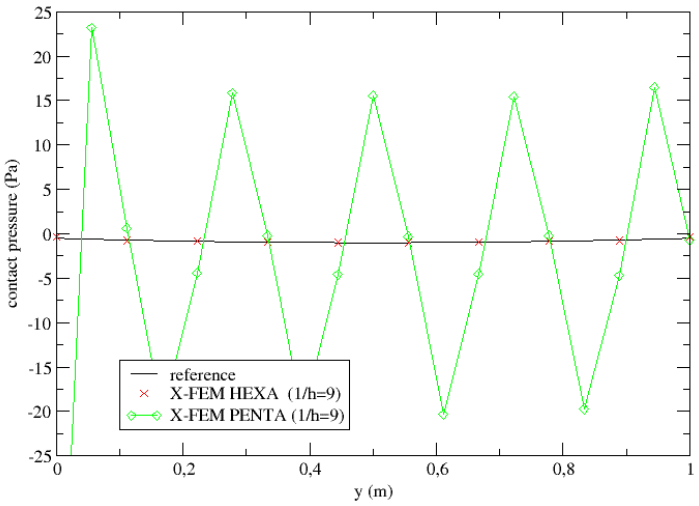


**Figure 5.** *Contact pressure oscillations.*

Let $E$ and $N$ be respectively the sets of all the edges and all the nodes of the mesh. The two vertices of an edge $e \in E$ are denoted by $(v_1(e),v_2(e)) \in N^2$. We define:

$$S_e = \left\{ e \in E, \quad \psi\left(v_1(e)\right) \cdot \psi\left(v_2(e)\right) < 0 \right\}$$

the set of edges that are strictly cut by the interface. The interface being represented by a level set function $\psi$, an edge $e \in E$ is strictly cut by the interface if $\psi(v_1(e)).\psi(v_2(e)) < 0$. Note that if the interface coincides with node $v_1(e)$ or node $v_2(e)$, the edge $e$ is not in $S_e$. Let $N_e$ be the set of nodes connected by the elements of $S_e$. We split $N_e$ in two parts: the nodes “below” and “above” the interface, depending on the sign of $\psi$:

$$N_e = \left\{ n \in N, \quad \exists e \in S_e \quad n = v_1(e) \quad \text{or} \quad n = v_2(e) \right\}$$
$$N_e^+ = \left\{ n \in N_e, \quad \psi(n) > 0 \right\} \quad \text{and} \quad N_e^- = \left\{ n \in N_e, \quad \psi(n) < 0 \right\}$$

The algorithm searches for $S_{ve}$, a minimal sub-set of $S_e$ which permits to connect nodes in $N_e^+$ to nodes in $N_e^-$. This set is not necessarily unique. If there is a choice between two edges, we keep the shortest one, aiming to minimize the P0 (constant) approximation area. Edges in $S_{ve}$ are called "vital edges", because if one of these edges is missing, at least one node in $N_e$ will be isolated on one side. It is important to notice that $S_{ve}$ is composed by some disconnected edges and some connected edges. Those groups of connected vital edges are extracted from $S_{ve}$. Note that in such a group, all the edges are connected by a unique node (See Figure 6). Let $G_{cve}^{\ i}$ be the group of vital edges connected by node $i$. $G_{cve}^{\ i}$ is defined by:

$$G_{cve}^{i} = \left\{ e \in S_{ve}, \quad i = v_1(e) \quad \text{or} \quad i = v_2(e) \right\}$$

Now, we impose the relations between the multipliers. All the multipliers linked to edges within a group are imposed to be equal. No relation is imposed on the Lagrange multipliers linked to single vital edges. These multipliers are free The other multipliers are on non-vital edges. They are not essential for the contact pressure approximation. Therefore we impose them to be a linear combination of multipliers on vital edges. These linear combinations are determined by the following procedure. Let $\lambda_e$, $e \in S_e \backslash S_{ve}$ be the Lagrange multiplier which lies on a non-vital edge $e$. For each vertex of the edge $e$, we search the closer (in terms of physical distance, not middle node distance) $\lambda_k$ lying on an edge connected to $e$:

$$\text{for } i = 1,2 \quad \text{find } k_i, \quad \text{dist}\left(\lambda_e, \lambda_{k_i}\right) = \min_k \left\{ \text{dist}\left(\lambda_e, \lambda_k\right), k \in G_{cve}^{v_i(e)} \right\}$$

The linear relation is imposed between $\lambda_e$, $\lambda_{k_1}$ and $\lambda_{k_2}$ :

$$\lambda_e = \frac{\text{dist}\left(\lambda_e, \lambda_{k_2}\right)}{\text{dist}\left(\lambda_e, \lambda_{k_1}\right) + \text{dist}\left(\lambda_e, \lambda_{k_2}\right)} \lambda_{k_1} + \frac{\text{dist}\left(\lambda_e, \lambda_{k_1}\right)}{\text{dist}\left(\lambda_e, \lambda_{k_1}\right) + \text{dist}\left(\lambda_e, \lambda_{k_2}\right)} \lambda_{k_2}$$

The main difference between the algorithm in (Moës *et al.*, 2005) denoted as algo1, and algorithm presented in this paper (algo2) resides in the choice of a representative geometrical feature. In algo1, the geometrical entities which will influence the building of the approximation spaces are nodes, denoted as "winner nodes" in (Moës *et al.*, 2005). We have thought that contact pressure is directly related to the edges, that is why in algo2, the geometrical entities which will influence the building of the approximation spaces are edges, called "vital edges".

To illustrate this algorithm, let us examine the 2D example of Figure 6. The vital edges are in plain line, and the non-vital edges are in dotted line. It can be noticed that edge {2-10} or edge {3-10} can be chosen as vital edges. But as we said before, we privilege the shortest edge to be a vital edge, so {2-10} $\in S_{ve}$ and not {3-10}.

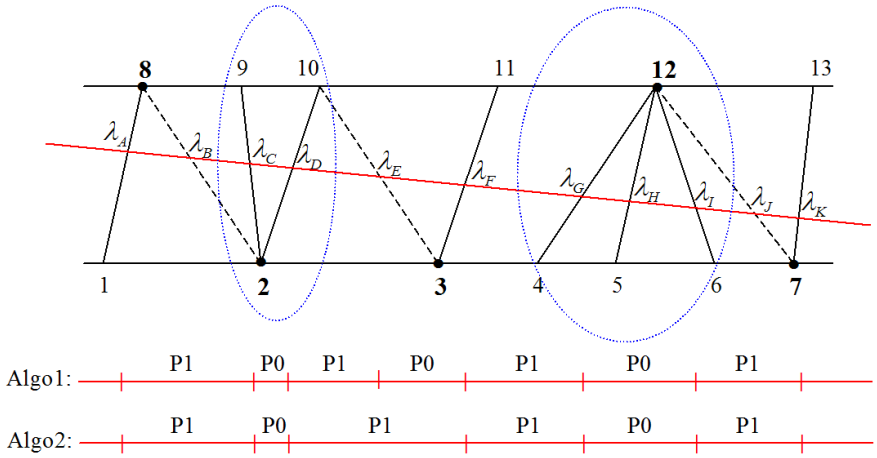


**Figure 6.** *Example of edges cut by an interface. Dotted edges are non-vital. Groups of connected vital edges are circled. The final multiplier approximation (P0 or P1) is plotted on the interface for both algorithms.*

Two groups of connected vital edges can be extracted (Figure 6). In each group, the multipliers are imposed to be equal. The three non-vital edges are {2-8}, {3-10} and {7-12}. For each one, a linear relation between the multipliers is imposed:

$$S_e = \{1-8; 2-8; 2-9; 2-10; 3-10; 3-11; 4-12; 5-12; 6-12; 7-12; 7-13\}$$
$$S_{ve} = \{1-8\,;\, 2-9\,;\, 2-10\,;\, 3-11\,;\, 4-12\,;\, 5-12\,;\, 6-12\,;\, 7-13\}$$
$$S_e \setminus S_{ve} = \{2-8\,;\, 3-10\,;\, 7-12\}$$
$$G_{cve}^{2} = \{2-9\,;\, 2-10\} \quad \text{and} \quad G_{cve}^{12} = \{4-12\,;\, 5-12\,;\, 6-12\}$$
$$\lambda_C = \lambda_D, \quad \lambda_G = \lambda_H = \lambda_I$$
$$\lambda_B = \frac{BC \cdot \lambda_A + AB \cdot \lambda_C}{AB + BC}, \quad \lambda_E = \frac{EF \cdot \lambda_D + DE \cdot \lambda_F}{DE + EF}, \quad \lambda_J = \frac{JK \cdot \lambda_I + IJ \cdot \lambda_K}{IJ + JK}$$

If we apply the algorithm of (Moës *et al.*, 2005), 5 winner nodes (nodes 8, 2, 3, 12, 7) will be found, represented by a dot on Figure 6. For both algorithms, the length of the Lagrange multiplier space is equal to 5. But if we compare the degrees of the approximation (P0 or P1) we notice that the P1 region is larger for algo2. This difference comes from a different choice of relations to be applied on $\lambda_E$: with algo1, $\lambda_E$ is imposed to be equal to $\lambda_F$ whereas with algo2 $\lambda_E$ is a linear combination of $\lambda_D$ and $\lambda_F$.

The above illustration shows a 2D example, but it is worth noticing that this algorithm is described indifferently in 2D/3D, and works in 2D or 3D without any modifications. Now we apply this algorithm to the case shown on Figure 4. We study the contact pressure on the interface as the mesh gets finer *i.e.* when the number of elements $1/h$ increases. Figure 7 shows that when this algorithm is used, the reduction of the contact pressure oscillations is quite effective. The convergence towards the analytical solution is observed. A comparison of both algorithms is given on Figure 8 for two different mesh densities. It seems that results obtained with algo2 are more accurate than the ones obtained with algo1. Several other tests have been carried out, and lead to conclude that algo1 tends to impose more equality relations whereas algo2 tends to impose more linear relations.

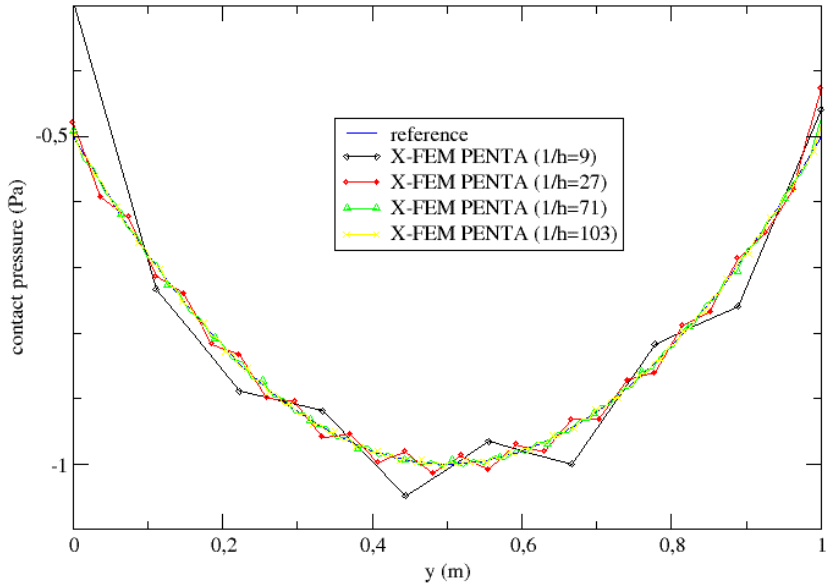


**Figure 7.** *Reduction of the contact pressure oscillations as the mesh gets finer.*

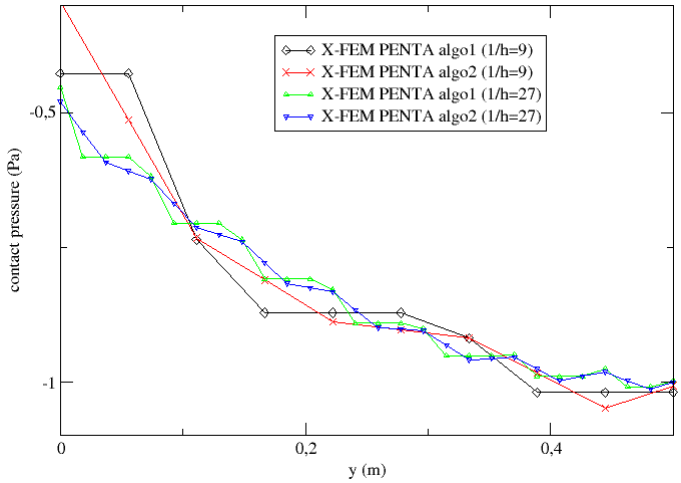


**Figure 8.** *Comparison of the contact pressure for both algorithms on half-length of the structure.*

As the LBB condition ensures optimal convergence, we verify the error convergence so as to check that the condition is respected. The error energy is defined by:

$$W\left(\mathbf{u}^{\mathbf{h}}\right)=\left(\frac{\int_{\Omega}\boldsymbol{\varepsilon}\left(\mathbf{u}^{\mathbf{h}}-\mathbf{u}^{\mathbf{ref}}\right):\mathbf{C}:\boldsymbol{\varepsilon}\left(\mathbf{u}^{\mathbf{h}}-\mathbf{u}^{\mathbf{ref}}\right)d\Omega}{\int_{\Omega}\boldsymbol{\varepsilon}\left(\mathbf{u}^{\mathbf{ref}}\right):\mathbf{C}:\boldsymbol{\varepsilon}\left(\mathbf{u}^{\mathbf{ref}}\right)d\Omega}\right)^{1/2}$$

Let ***n*** be the unit normal of the interface, a L2 norm error on the contact pressure is also defined by:

$$L\left(\lambda^{h}\right)=\left(\frac{\int_{\Gamma}\left(\lambda^{h}-\mathbf{n}\cdot\boldsymbol{\sigma}^{\mathbf{ref}}\cdot\mathbf{n}\right)^{2}d\Omega}{\int_{\Gamma}\left(\mathbf{n}\cdot\boldsymbol{\sigma}^{\mathbf{ref}}\cdot\mathbf{n}\right)^{2}d\Omega}\right)^{1/2}$$

We compare on Figure 9 the energy error convergence for FEM and X-FEM. With FEM, the mesh follows the interface. As expected, the hexahedron mesh with X-FEM gives the same convergence rate as the classical FEM with a conforming mesh. The slopes of the log-log curves are equal to -1. When considering a pentahedron mesh with both algorithms, the errors are higher for algo1 and algo2 but the same convergence rates are obtained.

A difference between the two algorithms is presented on Figure 10 where the L2 error norm on the contact pressure is plotted. From the slopes of log-log curves, it is

clear than the second algorithm gives slightly more accurate results. When no algorithm is used, the slope cannot be determined because the error on the contact pressure does not converge.

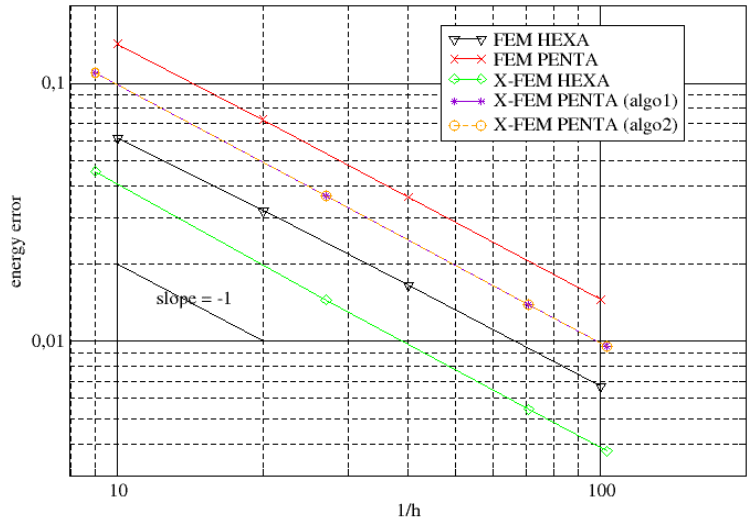


**Figure 9.** *Energy error convergence.*

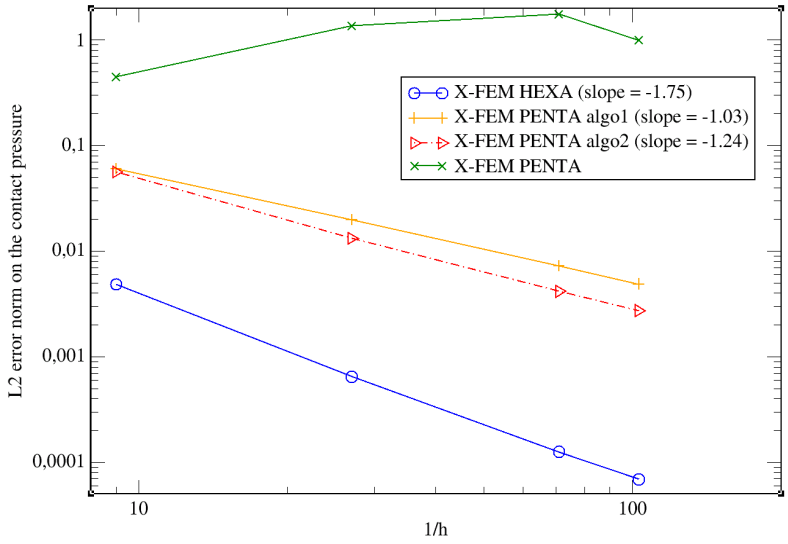


**Figure 10.** *L2 norm error norm on the contact pressure convergence.*

## 6. Conclusions

This paper has presented an original method to take into account contact aspects for the interface in the 3D X-FEM framework. This method is based on a mixed displacement-contact pressure variational formulation of the frictional contact problem derived from a continuous approach. We have focused on an implementation in a general finite element software. A study of different algorithms has been carried out to eliminate oscillations of the normal and tangential contact pressures in the case of adhesion linked to the satisfaction of the LBB condition.

Next steps will be dealing with frictional contact when sliding occurs and its extension to crack problems. Therefore, in addition to sliding, we are now investigating the contact aspects near the crack front, in the area where singular functions are added to the classical shape functions to take into account the singularity of the solution. This point is essential to perform realistic simulations of cracks in fatigue under cyclic loadings.

## 7. References

Alart P., Cunier A., “A mixed formulation for frictional contact problems prone to Newton like solution methods”, *Computer Methods in Applied Mechanics and Engineering*, 92, 1991, 353-375.

Bathe K.J., “The inf–sup condition and its evaluation for mixed element methods”, *Computers and Structures*, 79 (2001), 243-252

Béchet E., Minnebo H., Moës N., Burgardt B., “Improved implementation and robustness study of the X-FEM for stress analysis around cracks”, *International Journal for Numerical Methods in Engineering*, 64 (8), 1033-1056, 2005

Belytschko T., Moës N., Usui S. and Parimi C., “Arbitrary discontinuities in finite elements”, *International Journal for Numerical Methods in Engineering*, 50, 993-1013 (2001)

Ben Dhia H., “Modelling and numerical approach of contact and dry friction in simulation of sheet metal forming”, Proceedings of Second World Congress on Comput. Mech., Stuttgart, August 27-71, 1990, p.779-782

Ben Dhia H., Vautier I., “Une formulation pour traiter le contact frottement en 3D dans le Code_Aster”, Rapport de recherche HI-75/99/007/A, juin 1999, EDF R&D.

Ben Dhia H., Vautier I., Zarroug M., “Problèmes de contact frottant en grandes transformations: du continu au discret”, *Revue européenne des éléments finis*, vol.9, n°1-2-3, 2000, p. 243-261.

Ben Dhia H., Zarroug M., “Hybrid frictional contact particles-in elements”, *Revue européenne des éléments finis*, vol.11, n°2-4, 2002, p. 417-430.

Curnier A, He, Q.C., Klarbring A., “Continuum mechanics modelling of large deformation contact with friction”, Contact mechanics, ed. Plenum Press, 1995

Dolbow J., Moës N., Belytschko T., « An extended finite element method for modelling crack growth with frictional contact », *Computer Methods in Applied Mechanics and Engineering*, vol. 190, 2001, p. 6825-6846

Dumont G., Algorithme des contraintes actives et contact unilatéral sans frottement, *Journal européen des éléments finis*, 4(1), 55-73, 1995

Elguedj T., Gravouil A., Comberscure A., "Appropriate extended functions for X-FEM simulation of plastic fracture mechanics", *Computer Methods in Applied Mechanics and Engineering*, 195 (2006) 501-515

Fries T-P., Matthies H-G., "Classification and overview of Meshfree methods", informatikbericht Nr.: 2003-3, July, 2004

Gravouil A., Moës N., Belytschko T., "Non-planar 3D crack growth by the extended finite element and level sets - Part II: Level set update", *International Journal for Numerical Methods in Engineering*, 53, 2569-2586, 2002

Ji H., Dolbow J.E., "On strategies for enforcing interfacial constraints and evaluating jumps conditions with the extended finite element method", *International Journal for Numerical Methods in Engineering*, 61, 2508-2535, 2004

Laursen T.A., Simo J.C. "A continuum element-based formulation for the implicit solution of multi-body, large deformation frictional contact problem", *International Journal for Numerical Methods in Engineering*, 36, 3451-3485, 1993

Legrain G., Moës N., Verron E., "Stress analysis around crack tips in finite strain problems using the eXtended Finite Element Method", *International Journal for Numerical Methods in Engineering*, 63 (2), 290–314, 2005

Li S.C., Cheng Y.M., "Enriched meshless manifold method for two-dimensional crack modelling", *Theoretical and Applied Fracture Mechanics*, 44 (2005) 234–248

Melenk J.M., Babuška I., "The partition of unity finite element method: Basic theory and applications", *Computer Methods in Applied Mechanics and Engineering*, 139, 1999, 289-314.

Moës N., Dolbow J., Belytschko T., "A finite element method for crack growth without remeshing", *International Journal for Numerical Methods in Engineering*, 46, 1999, 131-150.

Moës N., Béchet E., Tourbier M., "Imposing essential boundary conditions in the X-FEM", *International Journal for Numerical Methods in Engineering*, 2005, accepted

Ribeaucourt R., Baietto-Dubourg M.C., Gravouil A., "Modèle numérique de propagation de fissures en fatigue de contact. Application à la fatigue de roulement". *7ème Colloque National en Calcul des Structures*, Giens (France),17-20/05/2005, Vol. 2, 641-646.

Sukumar N., Chopp D.L., Moës N., Belytschko T., "Modelling holes and inclusions by level sets in the extended finite-element method", *Computer Methods in Applied Mechanics and Engineering*, vol. 190, 2001, p. 6183-6200.

Zarroug M., "Éléments mixtes de contact frottant en grandes transformations et applications", Thèse de doctorat, École Centrale de Paris, 2002.